Supporting Information

Becker et al. 10.1073/pnas.1420308112

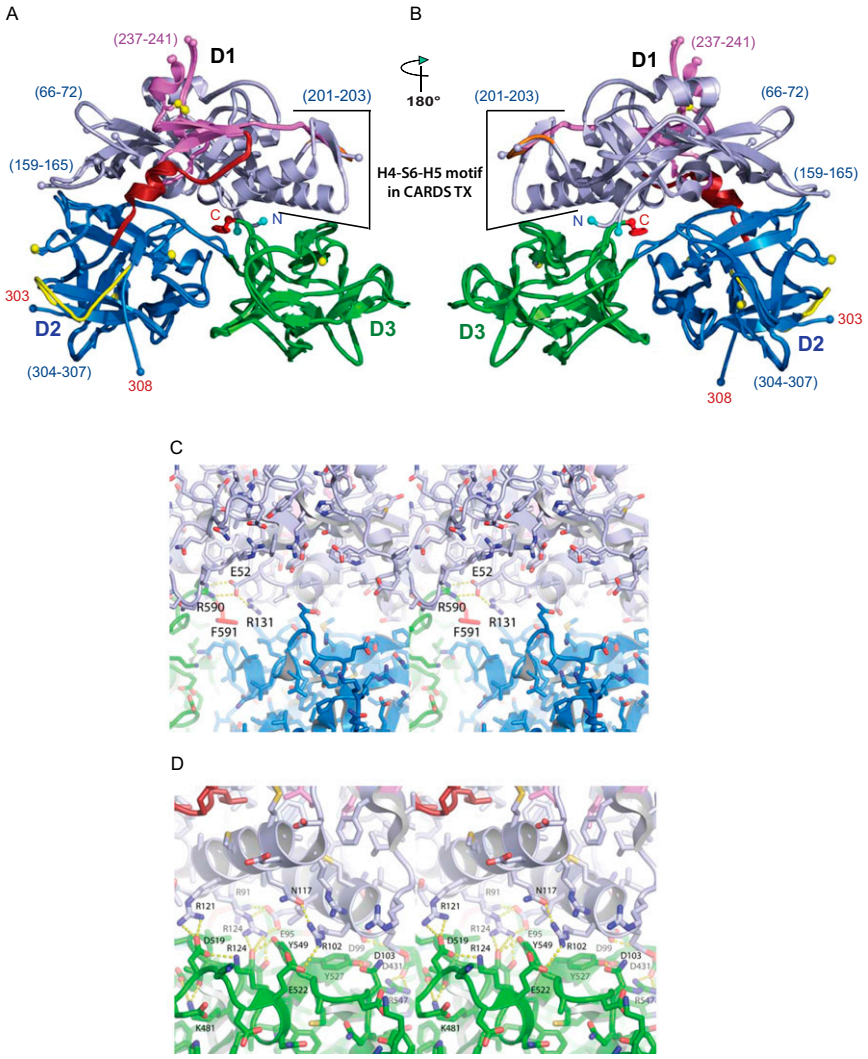

Fig. S1. "Native" and "nicked" CARDS TX structures and the interface beween D1 and D2+D3. The mART domain (residues 1–205) is light blue, the steric block of the NAD^+-binding site (residues 206–256) is violet, the linker connecting D1 to D2+D3 (residues 257–272) is dark red, D2 (residues 273–439) is dark blue, D3 (residues 440–591) is green, the loop in D2 containing the site of cleavage in limited trypsinolysis experiments (residues 303–314) is yellow, the sulfur atoms of Cys residues are yellow spheres, and the C-terminal residue F591 is bright red. (*A*) Superposition of native and nicked CARDS TX structures (rmsd 0.33 Å for 469 Cα pairs). Residues 66–72, 159–165, and 201–203 in D1 of the native structure are disordered. Residues 304–307 in the nicked CARDS TX structure are absent owing to trypsinolysis after K303 and K307. (*B*) Native CARDS TX structure superimposed on the nicked CARDS TX structure. The view is 180° around the vertical axis relative to *A*. The helix-strand-helix (H4-S6-H5) of the D1 mART domain that is unique to CARDS TX and interacts with D3 is indicated. (*C*) Divergent stereo pair showing the interface between D1 and D2. The interactions are tenuous, suggesting that disruption of the interactions between D1 and D3 may be sufficient to expose the catalytic residues and ARTT target recognition motif. (*D*) Divergent stereo pair showing the interface between D1 and D3. The interactions are primarily polar, and there are many interdomain hydrogen bonds and ion pairs. The two helices in the image are H4 and H5 from the H4-S6-H5 motif unique to CARDS TX.

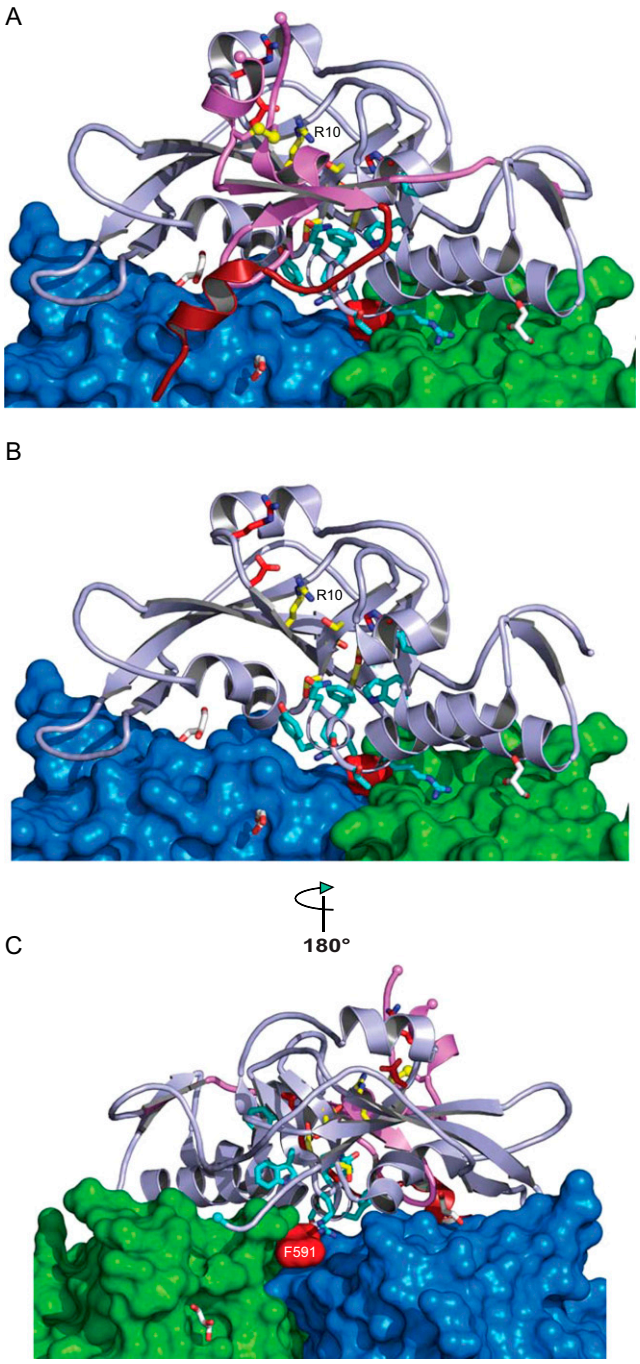

Fig. S2. Steric blocks of CARDS TX mART activity. The color code is the same as in Fig. S1. Active site residues are shown as sticks in the color scheme presented in the sequence alignment in Fig. 3*A*. Three glycerol molecules from the cryoprotectant are free-floating white and red sticks. (*A*) The steric block of the NAD^+-binding pocket consisting of residues 205–256 (violet). The flat surface of D2/D3 occludes residues of the ARTT motif involved in target protein recognition. (*B*) The steric block of the NAD^+-binding pocket and the linker connecting D1 to D2/D3 have been removed, permitting access to the NAD^+-binding pocket and residues of the ARTT target recognition motif (cyan). (*C*) F591 interacts with residues of the ARTT motif and active site.

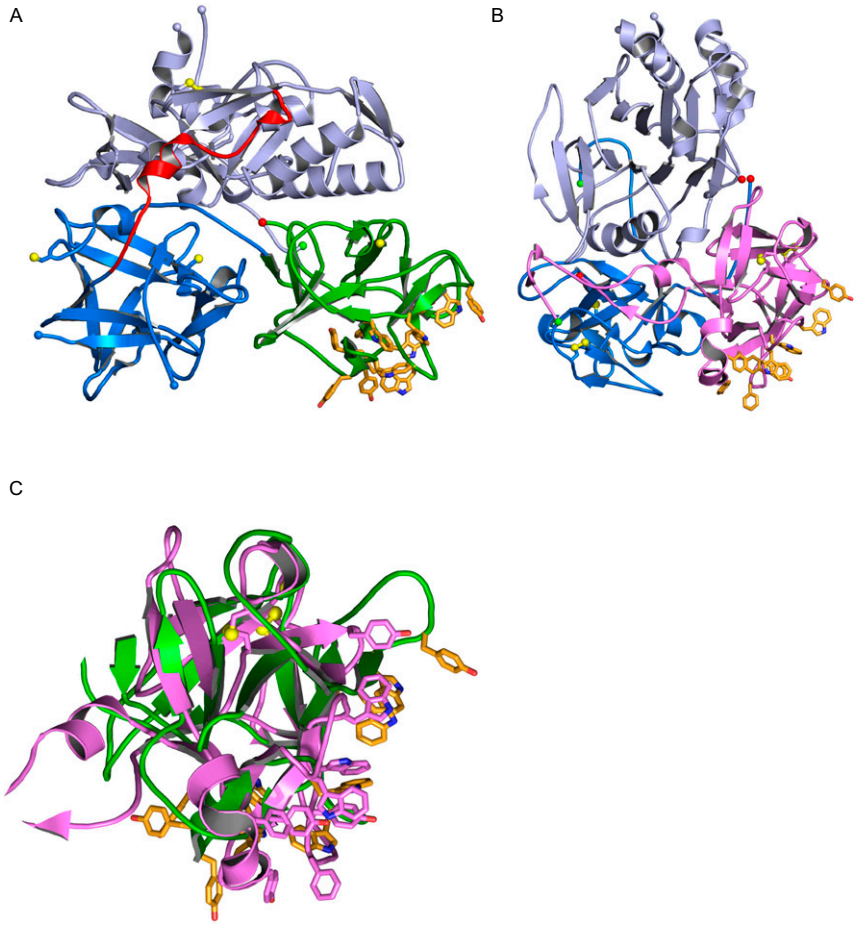

Fig. S3. Comparison of CARDS TX to CDT. The catalytic mART domain of CARDS TX and the nuclease domain of CDT are in light blue. (*A*) CARDS TX. Residues comprising the aromatic patch in D3 are shown as orange sticks. (*B*) CDT from *H. ducreyi* (PDB ID code 1SR4). Residues comprising the aromatic patch in CdtA are shown as orange sticks. The relative orientations of the β-trefoils in CARDS TX (dark blue and green) and CDTa (violet) and CDTc (blue) are similar. (*C*) CARDS TX D3 superimposed on CdtA. Residues of the aromatic patch in CdtA are violet sticks.

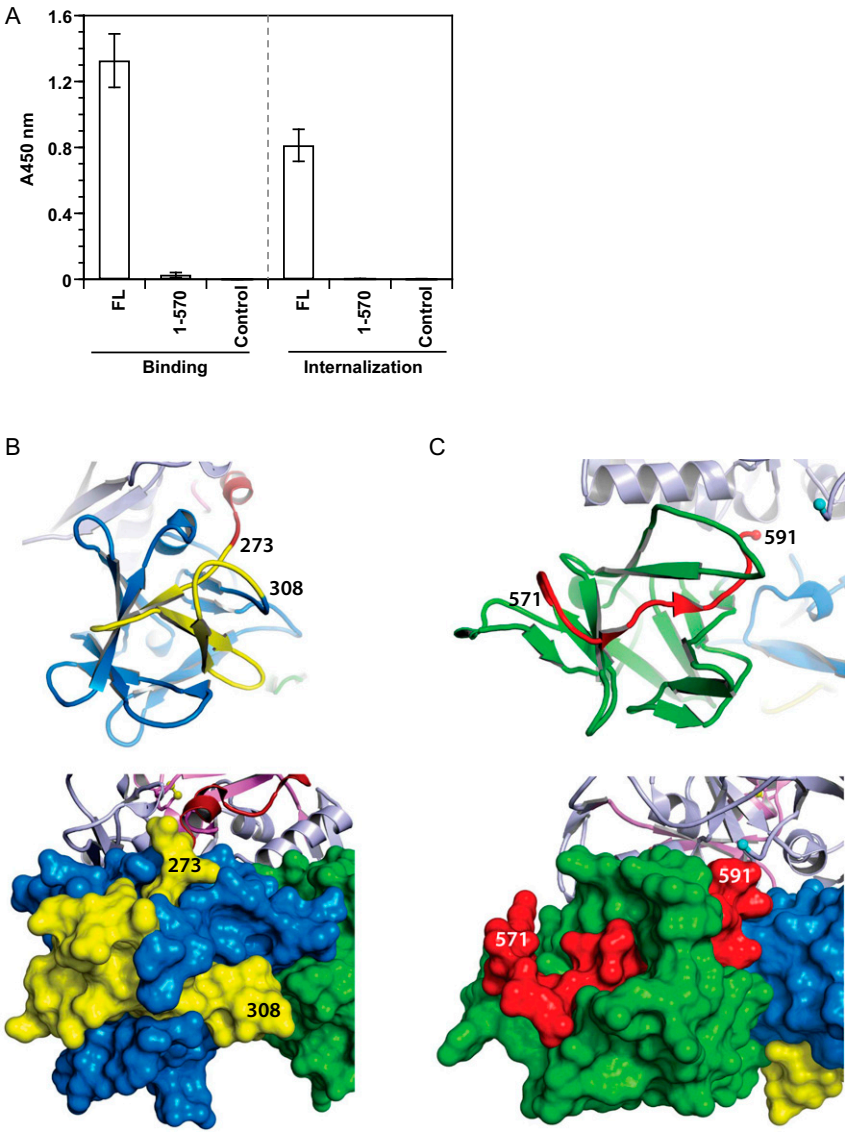

Fig. S4. CARDS TX cell surface binding and internalization by HeLa cells is mediated by D3. (*A*) Full-length CARDS TX consisting of residues 1–591 binds to and is internalized by HeLa cells, but a CARDS TX variant missing the C-terminal 20 amino acids neither binds nor is internalized. (*B*) Residues 273–308 of D2 are predicted to play a critical structural role in maintaining the fidelity of the D2 fold. These residues comprise one-third of the D2 beta trefoil. The view is down the pseudo-threefold axis of D2. (*C*) Residues 571–591 of D3 are predicted to play a critical structural role in maintaining the fidelity of the D3 fold. The results in *A*, taken together with previous work on the construct shown in *B*, indicate that binding and internalization of CARDS TX is mediated by D3.

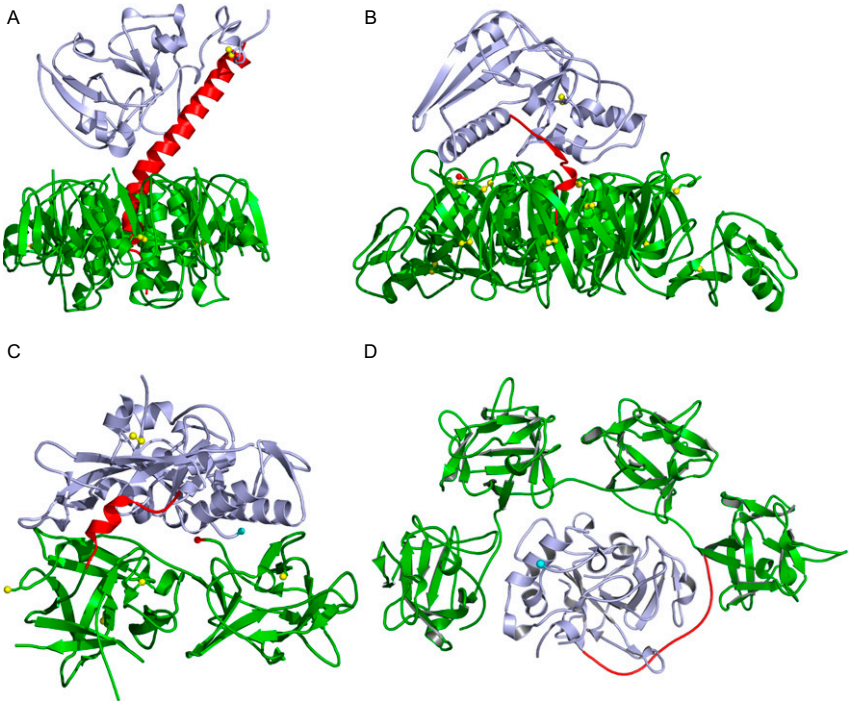

Fig. S5. CARDS TX architecture differs from other bacterial ADP-ribosylating toxins. Here mART domains are light blue, cell surface binding domains are green, linkers between mART and cell surface binding domains are red, and Cys Sγ atoms are yellow spheres. (*A*) Cholera toxin (PDB ID code 1xtc). (*B*) Pertussis toxin (PDB ID code 1prt). (*C*) CARDS TX (this study). (*D*) Mosquitocidal toxin (PDB ID code 2vse). The only toxins with both mART and β-trefoil domains are CARDS TX and mosquitocidal toxin, although the number and arrangement of β-trefoil domains relative to the mART domains is completely different in the two toxins.

Table S1. X-ray diffraction data and protein structure refinement statistics for CARDS TX in two crystal forms

	Native, nicked high-resolution	Native, unnicked	Native, nicked	Xenon derivative
Data collection				Phasing
PDB ID code	4TLV	4TLW		
Space group	*C*2	*R*3 [*H*3]*	*C*2	*C*2
Cell dimensions				
a, *b*, *c*, Å	191.7, 107.4, 222.3	107.3, 107.3, 107.3 [178.4, 178.4, 89.5]*	191.4, 107.4, 222.1	191.4, 107.2, 221.3
α, β, γ, °	90, 90.6, 90	112.6, 112.6, 112.6 [90, 90, 120]*	90, 90.6, 90	90, 90.4, 90
Wavelength, Å	0.9795	0.97903	1.5418	1.5418
Resolution, Å	50–1.9	50–2.55	30–2.2	30–2.7
R_{sym} †	0.073 (0.577)	0.059 (0.522)	0.077 (0.443)	0.099 (0.466)
$I/\sigma I$	15.5 (2.3)	20.5 (2.1)	13.1 (2.3)	10.2 (2.1)
Completeness, %	99.7 (100)	99.1 (93.2)	99.5 (99.7)	95.0 (92.1)
Redundancy	3.1 (3.2)	4.5 (4.1)	2.9 (2.8)	2.9 (2.8)
SIRAS phasing				
Resolution, Å	—	—		30.0–4.0 Å
R_{cullis} (iso/ano)	—	—		0.92/0.86
Phasing power (iso/ano)	—	—		0.66/0.82
Figure of merit	—	—		0.39
No. of xenon sites	—	—		27
Refinement				
Resolution, Å	38.87–1.9	44.61–2.55		
No. of reflections	350,157	34,124		
R_{work}/R_{free}	0.186/0.215	0.198/0.244		
No of atoms				
Protein	28,393	4,632		
Ligand	203	—		
Solvent	1,808	25		
B factors, Å^2				
Protein	27.1	77.8		
Ligand	29.1	—		
Solvent	27.8	59.9		
rmsd				
Bond length, Å	0.010	0.008		
Bond angle, °	1.099	1.102		

*Unit cell parameters for the *R3* crystal form on the hexagonal setting are in square brackets.
†Values in parentheses are for the highest-resolution shell.